

Low-temperature thermal conductivity of heavily doped *n*-type Ge

T. Sota and K. Suzuki

Department of Electrical Engineering, Waseda University, Shinjuku, Tokyo 160, Japan

D. Fortier*

Centre d'Etudes Nucléaires de Saclay, F-91190 Gif-sur-Yvette, France

(Received 14 November 1984)

We have theoretically studied the low-temperature thermal conductivity κ of heavily doped *n*-type Ge by using an expression of the phonon relaxation rate previously derived by us in which both the intravalley and intervalley relaxation times of the conduction electrons due to ionized impurities have been taken into account. We have measured κ of a Ge sample doped with 2.78×10^{18} As cm⁻³ at $1.2 < T < 7$ K. The following is found: In the temperature region $T < 1$ K, κ becomes more sensitive to the intervalley relaxation time as T decreases; that is, the dependence of κ on the impurity species becomes more pronounced. On the other hand, in the temperature region $T \gtrsim 2$ K, κ depends weakly on the impurity species. This seems to be consistent with the experimental data reported previously and given by us here. Furthermore, the calculated thermal conductivity is quantitatively in fairly good agreement with the experiment. However, there exist some discrepancies between them. A discussion on this is given.

I. INTRODUCTION

Since Fagen *et al.*¹ reported a large decrease of the thermal conductivity κ of Ge doped with 2.5×10^{18} Sb cm⁻³ at temperatures below 4 K, Pearlman and his collaborators^{2,3} have experimentally investigated κ of *n*-type Ge samples doped with various impurity species over the wide concentration region in the temperature region $T > 1.3$ K. The results for uncompensated samples at low temperatures may be summarized as follows. The thermal conductivity of lightly doped samples is very sensitive to the impurity species. On the other hand, κ of heavily doped samples exhibits only weak dependence on the impurity species.

The thermal conductivity of heavily doped *n*-type Ge where thermal phonons are strongly scattered by the conduction electrons has been previously analyzed by using Ziman's expression⁴ for the phonon relaxation rate, for example, in Refs. 2 and 5–8. Ziman's expression has been derived for a single valley under the conditions that both effects of electrons having a finite relaxation time and of screening the electron-phonon interaction can be neglected. Furthermore, in Refs. 5–8 germanium has been assumed to have a single valley, although, in fact, it has a many-valley structure. This leads to overestimation of the Fermi wave number k_F and, consequently, the cutoff wave number $q_c = 2k_F$ of the electron-phonon interaction, and to the failure to note that in a many-valley semiconductor the repopulation effect of electrons among valleys plays an important role in the phonon relaxation rate. Thus any appropriate analysis for κ of heavily doped *n*-type Ge has not yet been done.

Recently we have derived an expression for the phonon relaxation rate suitable for heavily doped many-valley semiconductors by solving the equation of motion for the single-particle density matrix within the self-consistent

and the relaxation-time approximations.^{9,10} (Hereafter Refs. 9 and 10 are referred to as I and II, respectively.) In this paper we will theoretically study the low-temperature thermal conductivity of heavily doped *n*-type Ge using the expression, and will give the experimental result of κ of an As-doped Ge sample with concentration 2.78×10^{18} cm⁻³.

II. PHONON RELAXATION RATE DUE TO CONDUCTION ELECTRONS

The processes of the phonon attenuation in heavily doped *n*-type Ge are summarized as follows. The conduction band of Ge has four equivalent valleys whose bottoms lie at *L* points in the first Brillouin zone. When germanium is heavily doped with shallow donor impurities, the electron system will be considered a degenerate electron gas at low temperatures and the number of electrons in each conduction-band valley is identical in the thermal-equilibrium state. When an acoustic wave propagates through the crystal, it disturbs the electron system; in particular the equivalence of conduction-band valleys is destroyed due to strain associated with it, leading to the deviation of the electron population in each valley from the thermal-equilibrium value. The modified electron population relaxes toward an instantaneous local equilibrium value under perturbation through collision processes consisting of both the intravalley and the intervalley scattering. Here collision processes are dominated by impurity scattering at low temperatures. The acoustic wave loses its energy through the above-mentioned electronic processes. It should be noted that charges arising from the modified electron population induce a field which may cancel partially or completely the electron-phonon interaction, i.e., the interaction potential between the electron and the acoustic wave is not an external bare potential but a screened one. Therefore the problem should be

solved self-consistently.

In Refs. 5–8, where Ziman's expression has been used for the phonon attenuation, the circumstances mentioned above have not been taken into account at all. We have derived, in I, the phonon relaxation rate suitable for heavily doped many-valley semiconductors by solving the equation of motion for the single-particle density matrix within the self-consistent and the relaxation-time approximations. The results for the single-mode phonon relaxation rate, which are applicable to n -type Ge, are given by

$$\frac{1}{\tau_{e-ph}(\mathbf{q}, \lambda)} = -\frac{\omega}{\rho_m v_\lambda^2} \text{Im} \left[\sum_{i,j} C_{i,\lambda} R_{ij} C_{j,\lambda} \right], \quad (1)$$

where

$$R_{ij} = \chi_{ij} + \frac{v \sum_m \chi_{im} \sum_n \chi_{nj}}{1 - v \sum_{m,n} \chi_{mn}}, \quad (2)$$

$$C_{i,\lambda} = (\Xi_d + \frac{1}{3} \Xi_u) \hat{\mathbf{e}}_\lambda \cdot \hat{\mathbf{q}} + (\frac{1}{3} \Xi_u) \hat{\mathbf{e}}_\lambda \cdot [\underline{U}^{(i)} - \underline{1}] \cdot \hat{\mathbf{q}}, \quad (3)$$

with

$$\chi_{ij} = (A^{-1}B)_{ij}, \quad (4)$$

$$A_{ii} = \frac{\Gamma_i / \Lambda_i - i\omega\tau}{1 - i\omega\tau} + \frac{1 - \Gamma_i / \Lambda_i}{1 - i\omega\tau} \sum_{j \neq i} \frac{\Lambda_j}{\Lambda_i + \Lambda_j} \gamma' \tau, \quad (5)$$

$$A_{ij} = -\frac{1 - \Gamma_i / \Lambda_i}{1 - i\omega\tau} \frac{\Lambda_i}{\Lambda_i + \Lambda_j} \gamma' \tau \quad (i \neq j), \quad (6)$$

$$B_{ii} = \Gamma_i + \frac{1 - \Gamma_i / \Lambda_i}{1 - i\omega\tau} \sum_{j \neq i} \frac{\Lambda_i \Lambda_j}{\Lambda_i + \Lambda_j} \gamma' \tau, \quad (7)$$

$$B_{ij} = -\frac{1 - \Gamma_i / \Lambda_i}{1 - i\omega\tau} \frac{\Lambda_i \Lambda_j}{\Lambda_i + \Lambda_j} \gamma' \tau \quad (i \neq j), \quad (8)$$

$$\Lambda_i = \sum_{\mathbf{k}} \frac{f(E_{i,\mathbf{k}+\mathbf{q}}) - f(E_{i,\mathbf{k}})}{E_{i,\mathbf{k}+\mathbf{q}} - E_{i,\mathbf{k}}}, \quad (9)$$

$$\Gamma_i = \sum_{\mathbf{k}} \frac{f(E_{i,\mathbf{k}+\mathbf{q}}) - f(E_{i,\mathbf{k}})}{E_{i,\mathbf{k}+\mathbf{q}} - E_{i,\mathbf{k}} - \hbar\omega - i\hbar/\tau}, \quad (10)$$

$$f(E_{i,\mathbf{k}}) = \{1 + \exp[\beta(E_{i,\mathbf{k}} - \mu)]\}^{-1}, \quad (11)$$

$$v = 4\pi e^2 / (\epsilon_0 q^2), \quad (12)$$

$$\underline{U}^{(i)} = 3\mathbf{K}^{(i)}\mathbf{K}^{(i)}. \quad (13)$$

Here ω is the angular frequency of phonons with the wave vector \mathbf{q} ; ρ_m is the mass density of crystal; v_λ is the sound velocity for the polarization direction with $\lambda = 1, 2$, and 3, where $\lambda = 1$ stands for longitudinal, 2 and 3 for transverse modes; R_{ij} represents a component of density response functions; i, j, m , and n denote valley indices; $C_{i,\lambda}$ is the deformation potential for the electrons in the i th valley; τ and γ' , which depend on the impurity species, are, respectively, the total relaxation time and the intervalley relaxation rate of the electrons; \mathbf{k} is the wave vector of the electrons; $\beta = 1/k_B T$; μ is the chemical potential in the thermal equilibrium state; Ξ_d and Ξ_u are, respectively, the dilational and the shear components of the deformation potential constants; $\hat{\mathbf{e}}_\lambda$ is the polarization vector; $\hat{\mathbf{q}}$ is the unit vector along \mathbf{q} ; $\underline{1}$ is the 3×3 unit matrix; and $\mathbf{K}^{(i)}$ is

the unit vector pointing from the origin to the i th valley in the first Brillouin zone. The explicit expressions for Λ_i and Γ_i at $T = 0$ K obtained under the assumption that the rigid band is applicable have been given in I and II.

The phonon relaxation rate has usually been averaged over the solid angle to make calculations of the thermal conductivity feasible. Here we will also use this approximation. The angular-averaged phonon relaxation rate is obtained by

$$\frac{1}{\bar{\tau}_{e-ph}} = \frac{1}{4\pi} \int \int \frac{1}{\tau_{e-ph}(\mathbf{q}, \lambda)} \sin\theta d\theta d\phi, \quad (14)$$

where θ and ϕ represent the polar and the azimuthal angles. The energy surfaces of conduction-band valleys in many-valley semiconductors such as Ge are spheroidal, i.e., there exists the mass anisotropy. In this case calculations of the phonon relaxation rate denoted by $1/\bar{\tau}_{AI}$ must be done numerically using Eqs. (1)–(14) because the double integral in Eq. (14) cannot be performed analytically. On the other hand, when an isotropic effective mass is assumed we obtain the following expressions for the angular-averaged phonon relaxation rate:

$$\frac{1}{\bar{\tau}_0} = -\frac{\omega}{\rho_m \bar{v}_\lambda^2} \text{Im}[nR_D(\Xi_d + \frac{1}{3}\Xi_u)\delta_{1,\lambda} + R_S\Xi_u^2 \bar{U}_\lambda^2], \quad (15)$$

where

$$R_D = \frac{\Gamma}{F_1 - (n-1)F_2 - v\Gamma}, \quad (16)$$

$$R_S = \frac{\Gamma + n\Lambda F_2}{F_1 + F_2}, \quad (17)$$

$$F_1 = \frac{\Gamma/\Lambda - i\omega\tau}{1 - i\omega\tau} + \frac{(n-1)\gamma'\tau}{2(1 - i\omega\tau)} (1 - \Gamma/\Lambda), \quad (18)$$

$$F_2 = \frac{\gamma'\tau}{2(1 - i\omega\tau)} (1 - \Gamma/\Lambda), \quad (19)$$

$$\bar{U}_1^2 = \frac{16}{45}, \quad \bar{U}_2^2 = \frac{32}{135}, \quad \bar{U}_3^2 = \frac{8}{27}. \quad (20)$$

Here \bar{v}_λ is the averaged sound velocity for polarization direction λ , $n = 4$ for Ge and $\Lambda_i = \Lambda$ and $\Gamma_i = \Gamma$ for all $i = 1$ to 4; see I.

III. LATTICE THERMAL CONDUCTIVITY

First we will give a brief description on the experiment done for an As-doped Ge sample As1 whose characteristics are given in Table I. The impurity concentration was determined from the Hall coefficient at room temperature. The dislocation density of the sample was $4 \times 10^3 \text{ cm}^{-2}$. The thermal conductivity was measured using the longitudinal steady-state heat-flow technique at $1.2 < T < 7$ K. The long axis of the sample was along the [111] direction.

The thermal conductivity κ will be calculated by using the semiphenomenological expression¹¹

$$\kappa = \frac{k_B^4 T^3}{6\pi^2 \hbar^3} \sum_{\lambda} \frac{1}{\bar{v}_\lambda} \int_0^\infty \frac{x^4 e^x}{(e^x - 1)^2} \bar{\tau} dx, \quad (21)$$

with

TABLE I. Values of the physical parameters used in numerical calculations.

	As226	As1	P9	Sb222	Sb30
ρ_m (g cm ⁻³)			5.35		
\bar{v}_1 (10 ⁵ cm sec ⁻¹)			5.37		
$\bar{v}_2 = \bar{v}_3$ (10 ⁵ cm sec ⁻¹)			3.28		
Ξ_u (eV)			16		
Ξ_d (eV)			-10		
m^*/m_0			0.22		
m_l/m_0			1.58		
m_t/m_0			0.082		
ϵ_0			15.4		
N (10 ¹⁷ cm ⁻³)	8.8 ^a	27.8	11 ^b	11 ^a	25 ^a
L (cm)	0.46 ^a	0.27	0.45 ^b	0.45 ^a	0.25 ^a
τ (10 ⁻¹³ sec)	1.0 ^a	0.67	1.9 ^b	1.7 ^a	1.39 ^a
γ' (10 ¹¹ sec ⁻¹) ^c	20	30	10	0.5	0.5
A^* (10 ⁻⁴⁴ sec ³) ^c	4.5	6.0	5.0	5.0	6.0

^aReference 2.^bReference 3.^cSee text.

$$1/\bar{\tau} = 1/\tau_B + 1/\tau_I + 1/\bar{\tau}_{e-ph} \quad \text{and} \quad x = \hbar\omega/k_B T. \quad (22)$$

Here $1/\tau_B = \bar{v}_\lambda/L$ is the phonon relaxation rate due to the boundary scattering and L is Casimir's length. $1/\tau_I = A^*\omega^4 = A^*(k_B/\hbar)^4 T^4 x^4$ represents the phonon relaxation rate by Rayleigh scattering due to ionized donors and isotopes. Here A^* has been estimated according to Ref. 12. The phonon relaxation rate due to the electron-phonon interaction $1/\bar{\tau}_{e-ph}$ has the temperature dependence through the Fermi-Dirac distribution function f . However, since the temperature range of interest here is $T < 5$ K and the values of \hbar/τ are larger than 40 K the effect of finite temperature can be neglected, where the values of the total relaxation time τ of the conduction electrons are given in Table I. We use the expression for $1/\bar{\tau}_{e-ph}$ at $T=0$ K.

In numerical calculations of κ , the values of physical parameters given in Table I are used where m^* , m_l , and m_t are, respectively, the density-of-states, the longitudinal, and the transverse effective masses, and m_0 is the free-electron mass. The values of concentration N of Sb, As, and P have been chosen to compare the theory and the experiment reported previously^{2,3} and given by us later on. The values of τ have been determined from the electrical resistivity. The values of γ' for Sb and As donors have been determined from the intervalley relaxation time obtained by Mason and Bateman,¹³ while the value for P donors has been obtained assuming that the scattering strength is proportional to the square of the magnitude of the valley-orbit splitting.^{13,14}

The calculated results at $1 \leq T \leq 5$ K are shown in Fig. 1 where the values of concentration N used correspond to those of samples No. Sb30, No. Sb222, and No. As226 by Goff and Pearlman,² No. P9 by Mathur and Pearlman,³ and No. As1 by us. In Fig. 2 the results at $0.1 \leq T \leq 1$ K are shown for samples No. Sb222, No. As226, and No. P9 whose concentration is almost the same. In Figs. 1 and 2 solid lines represent the conductivity κ_0 obtained by using $1/\bar{\tau}_0$, and dotted lines represent that obtained by taking account of the boundary scattering alone.

From Figs. 1 and 2 the results are summarized as follows. At $T \geq 2$ K, κ_0 shows only weak dependence on the impurity species and is chiefly determined by N . The larger N leads to the smaller κ_0 . At $T \sim 1$ K, κ_0 depends on τ , γ' , and N , and the γ' dependence is the strongest. The shorter τ leads to the smaller κ_0 provided that the values of other physical parameters are fixed. Similarly the larger γ' leads to the larger κ_0 and the larger N leads to the smaller κ_0 . The dependence of κ_0 on γ' becomes clearer as T decreases at $0.1 \leq T < 1$ K. The smaller γ' leads to the smaller κ_0 . Note that in lightly doped samples the impurity-species dependence of κ arises from the difference in the valley-orbit splitting.

In order to make the behavior of κ_0 clear, as an example, we have shown the frequency (ω) dependence of $1/\bar{\tau}_0$ by solid lines, for $\lambda=3$ in samples No. Sb222 and No. P9 whose concentrations are identical, in Fig. 3 where the arrow indicates the cutoff frequency ω_c in the electron-phonon interaction. The reason for the choice of $\lambda=3$ is that the heat is mainly carried by transverse phonons and $1/\bar{\tau}_0$ for $\lambda=2$ and 3 are the same with regard to the ω dependence.

It can be seen from Fig. 3 that $1/\bar{\tau}_0$ becomes more sensitive to the values of γ' in the low-frequency region but it is not sensitive to those in the high-frequency region. Thus the dependence of κ_0 on the impurity species becomes more clear at lower temperatures, while it is weak at higher temperatures.

Next we consider the N dependence of $1/\bar{\tau}_0$ assuming that the values of γ' and τ are fixed. Let the subscripts 1 and 2 denote the higher and the lower concentration, i.e., $N_1 > N_2$. Although the results for $1/\bar{\tau}_{01}$ and $1/\bar{\tau}_{02}$ in this case are not shown here, the relations $1/\bar{\tau}_{01} > 1/\bar{\tau}_{02}$ at $\omega > \omega_{c2}$ and $1/\bar{\tau}_{01} \sim 1/\bar{\tau}_{02}$ at $\omega < \omega_{c2}$ are satisfied. Here the former reflects the fact that ω_c shifts to the higher values with increasing N . Therefore the larger N leads to the smaller κ_0 at higher temperatures, while at lower temperatures the N dependence of κ_0 is weak.

When the electrons have a finite relaxation time τ , $1/\bar{\tau}_0$ has a finite value even in $\omega > \omega_c$. Thus κ_0 calculated by using $1/\bar{\tau}_0$ with τ finite is much smaller than that with τ infinite. Let us consider the τ dependence of κ_0 assuming that the values of γ' and N are fixed. In this case the shorter τ leads to the larger $1/\bar{\tau}_0$; see Fig. 1(b) in I. Therefore the shorter τ leads to the smaller κ_0 .

The calculated curves of κ_0 are qualitatively consistent with the experimental data which are shown in Fig. 1 by dashed curves. Taking into account that no adjustable parameters have been used in calculations, agreement between the theory and experiment is quantitatively also fairly good. However, it should be also pointed out that there exist some discrepancies between them.

IV. DISCUSSIONS

First, we will make a few comments on the experiment. The concentration dependence of κ for Sb-doped Ge is similar to that for As-doped Ge, but that for P-doped Ge is not known since there is only one sample in the concentration region under consideration. The temperature dependence of κ of sample No. P9 at higher temperatures

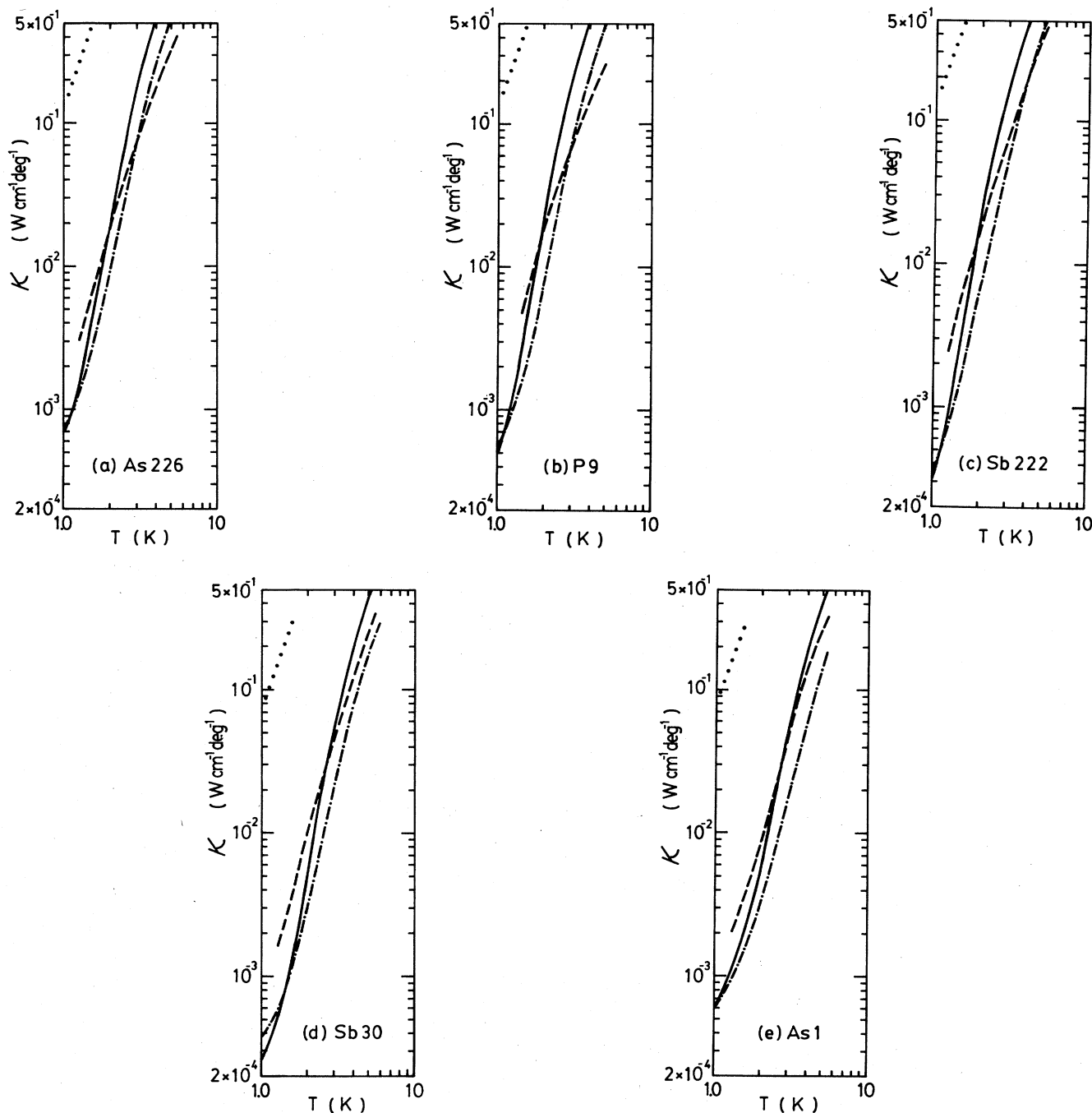


FIG. 1. Thermal conductivity obtained by the theory and the experiment for samples (a) No. As226, (b) No. P9, (c) No. Sb222, (d) No. Sb30, and (e) No. As1 at $1 \leq T \leq 5$ K. Dashed curves denote the experimental data for samples No. As226, No. Sb222, and No. Sb30 by Goff and Pearlman (Ref. 2), for samples No. P9 by Mathur and Pearlman (Ref. 3), and No. As1 by us. Solid and dotted-dashed curves represent the calculated results by using $1/\bar{\tau}_0$ and $1/\bar{\tau}_{AB}$, respectively. Dotted lines show the calculated results by using $1/\tau_B$ alone.

is slightly different from that of other samples, i.e., κ has a smaller exponent of T in the former than in the latter. The concentrations of all the samples given in Table I are determined by the Hall coefficient.¹⁵ It is known that the concentration obtained using this method is different from that obtained using the Irvin curve.¹⁶ Therefore there exists some ambiguity about the true concentration

of samples. For samples No. As226, No. P9, and No. Sb222 whose concentration is almost the same we have the relation $\tau(P) > \tau(Sb) \gtrsim \tau(As)$ for the total relaxation time of the conduction electrons. However, the relation $\tau(As) < \tau(P) < \tau(Sb)$ should be satisfied because the intervalley scattering strength, which contribute to τ , is determined by the short-range part of impurity potential which

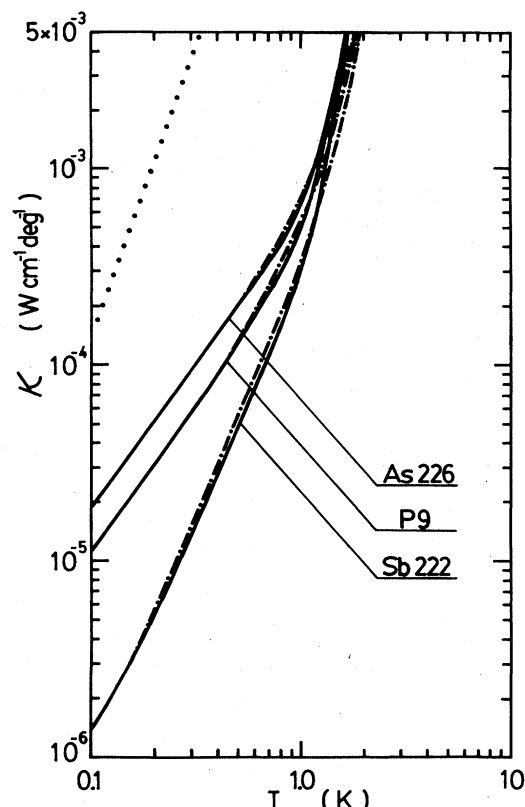


FIG. 2. Calculated results of the thermal conductivity for samples No. As226, No. P9, and No. Sb222 at $0.1 \leq T \leq 1$ K. Solid and dotted-dashed curves represent the calculated results by using $1/\tau_0$ and $1/\tau_{AI}$, respectively. Dotted line shows the calculated result by using $1/\tau_B$ alone.

causes the central-cell correction or the valley-orbit splitting for the neutral donors and that of Sb is the smallest. The dislocation density of our sample No. As1 is about $4 \times 10^3 \text{ cm}^{-2}$, while that of other samples is not given. Although we will be able to have a better fit by adjusting the values of the physical parameters within the allowed range due to uncertainty of them, the discrepancy cannot be resolved completely even using such adjusted values and, therefore, we have used the values given in Table I.

Next we discuss some other factors which might diminish the discrepancy between the theory and the experiment. It has been found in II that when phonons propagate along the principal axes the mass anisotropy of the conduction electrons has a remarkable influence on the phonon relaxation rate $1/\tau_{e-ph}(q, \lambda)$. Therefore in order to see to what degree the thermal conductivity κ is affected by the mass anisotropy, calculations of κ have been done using Eqs. (14) for $1/\tau_{AI}$ and (15) for which κ is denoted by κ_{AI} . Here it should be mentioned that the accuracy of numerical calculations of κ_{AI} is not so good as that of κ_0 .¹⁷ The results of κ_{AI} are shown in Figs. 1 and 2 by dotted-dashed curves and those of $1/\tau_{AI}$, as an example, for $\lambda=3$ in samples No. Sb222 and No. P9 are shown by dashed curves in Fig. 3. As can be seen from Fig. 1, agreement between the theory and the experiment is not improved. In order to obtain a better agreement between

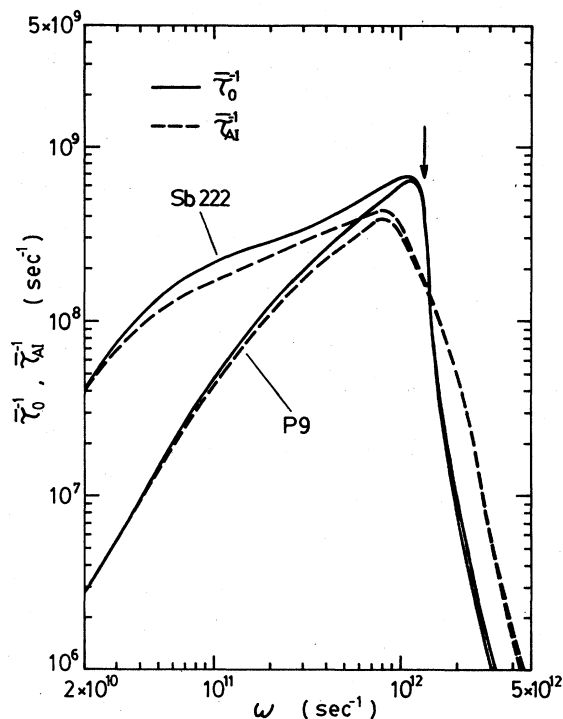


FIG. 3. Frequency dependence of the phonon relaxation rate for the polarization direction $\lambda=3$ for samples No. P9 and No. Sb222 where solid and dashed curves correspond to $1/\tau_0$ and $1/\tau_{AI}$.

them in the framework of an idealized electron system in which the rigid band is assumed, we will have to use the deformation potential which depends on the wave number, the concentration, and the impurity species. However, we do not know the reason why this should be so.

We examine the effect of internal stresses due to dislocation and charged impurities and unintentional external stresses. Calculations of the thermal conductivity performed have assumed, for simplicity, an isotropic effective mass and a uniaxial compressional stress applied along the [111] direction.¹⁸ The reason why the latter is assumed is that it decreases the phonon relaxation rate in the lower-frequency region and, consequently, is expected to decrease the discrepancy at lower temperatures. Although the calculated results are not shown here, we need the stress of about $2 \times 10^9 \text{ dyn/cm}^2$, for example, in sample No. Sb30 to obtain agreement. This magnitude of stress is unrealistic.

In conclusion, our theoretical calculations show that the dependence of the thermal conductivity on the impurity species becomes more pronounced as T decreases at $T < 1$ K. This is consistent with the results of the ultrasonic attenuation measurement for As- and Sb-doped Ge by Mason and Bateman.¹³ On the other hand, when Ziman's expression for the phonon relaxation rate is used, the impurity-species dependence of the thermal conductivity does not appear. In order to verify the theory presented herein, it will be desirable to perform the measurement of the thermal conductivity at $T < 1$ K.¹⁹

ACKNOWLEDGMENTS

The measurement of the thermal conductivity was done by one of the authors (D.F.) at Centre d'Etudes Nucléaires de Saclay. We are grateful to Professor Albany for his encouragement. We wish to express our appreciation to M.

Yawata and D. Uehara for their helpful assistance in numerical calculations. This work was supported in part by the Grant-in-Aid for "Special Project: Research on Ultrasonic Spectroscopy and Its Application to Material Science" from the Ministry of Education, Science and Culture.

*Present address: Laboratoire de Biophysique, Faculté de Médecine, Necker-Enfants-Malades, Paris 15, France.

¹E. Fagen, J. F. Goff, and N. Pearlman, *Phys. Rev.* **94**, 1415 (1954).

²J. F. Goff and N. Pearlman, *Phys. Rev.* **140**, A2151 (1965).

³M. P. Mathur and N. Pearlman, *Phys. Rev.* **180**, 833 (1969).

⁴J. M. Ziman, *Philos. Mag.* **1**, 191 (1956).

⁵N. K. S. Gaur and G. S. Verma, *Phys. Rev.* **159**, 610 (1967).

⁶K. C. Sood and G. S. Verma, *Phys. Rev. B* **5**, 3165 (1972).

⁷M. P. Singh and G. S. Verma, *Physica* **62**, 627 (1972).

⁸H. H. Boghosian and K. S. Dubey, *Phys. Status Solidi B* **88**, 417 (1978).

⁹T. Sota and K. Suzuki, *J. Phys. C* **15**, 6991 (1982).

¹⁰T. Sota and K. Suzuki, *J. Phys. C* **16**, 4347 (1983).

¹¹A. Griffin and P. Carruthers, *Phys. Rev.* **131**, 1976 (1963).

¹²V. V. Kosarev, P. V. Tamarin, and S. S. Shalyt, *Phys. Status Solidi B* **44**, 525 (1971).

¹³W. P. Mason and T. B. Bateman, *Phys. Rev.* **134**, A1387 (1964).

¹⁴P. J. Price and R. L. Hartman, *J. Phys. Chem. Solids* **25**, 567 (1964).

¹⁵M. Cuevas and H. Fritzsche, *Phys. Rev.* **139**, A1628 (1965).

¹⁶S. M. Sze and J. C. Irvin, *Solid-State Electron.* **11**, 599 (1968).

¹⁷The triple integral must be performed numerically to obtain κ_{AI} ; see Eqs. (14) and (21). However, to save computer time the following method has been used. We obtained $1/\tau_{AI}$ by performing the double integral in Eq. (14) numerically and approximated it by an appropriate simple function of ω .

¹⁸The procedure of deriving the averaged phonon relaxation rate $1/\bar{\tau}(X)$ under the condition that the stress is applied along the [111] direction is as follows. In this case, since the Fermi wave number in [111] valley is different from that in other valleys, Λ_i and Γ_i in the former must be distinguished from those in the latter. Taking this into account and using Eqs. (1)–(14), $1/\bar{\tau}(X)$ can be obtained after simple but tedious calculations.

¹⁹The electronic contribution to the measured thermal conductivity might not be negligible. Assuming that the Wiedemann-Franz law is applicable to the present system, the electronic thermal conductivity for 10^{18} cm^{-3} impurity concentration is about 10^{-7} W/cm deg at $T=0.1 \text{ K}$. It will be about 10% of the lattice thermal conductivity for Sb donors and 1% for As and P donors. It is expected to be negligible as the first approximation.